Energy Transfer and Spectral Dynamics of the Three Lowest Energy Q_y-States of the Fenna-Matthews-Olson Antenna Complex

M. Rätsep,[†] R. E. Blankenship,[‡] and G. J. Small*,[†]

Ames Laboratory-USDOE and Department of Chemistry, Iowa State University, Ames, Iowa 50011, and Department of Chemistry and Biochemistry, Arizona State University, Tempe, Arizona 85287-1604

Received: March 17, 1999; In Final Form: May 4, 1999

Temperature-dependent (1.8−10 K) spectral hole burning results are presented for the three lowest Q_y-states of the Fenna-Matthews-Olson (FMO) bacteriochlorophyll *a* antenna complex of *Chlorobium tepidum* that contribute to the 825 nm absorption band. Both holewidth and hole growth kinetic data are presented. The data indicate that the three states lie at 823, 825, and 827 nm and, furthermore, that they are associated with the lowest energy state of the subunit of the FMO trimer. Structural heterogeneity results in the three states being energetically inequivalent. The time constants for downward energy transfer from the 823 and 825 nm states are 37 and 117 ps, respectively. It is argued that the time constants for the 823 nm → 825 and 823 nm → 827 nm pathways are 117 and 54 ps, respectively. The dispersive hole growth kinetic data for the three states obtained at 1.8 and 9.0 K are shown to be consistent with the excited-state lifetimes and homogeneous widths of the zero-phonon absorption lines. Analysis of the data leads to a lifetime of 2 ns for the 827 nm state. The temperature dependencies of the zero-phonon lines associated with this and the other two states are identical and characteristic of coupling to the two-level systems of the protein.

1. Introduction

The Q_y-electronic structure and excitation energy transfer (EET) dynamics of the Fenna-Matthews-Olson (FMO) bacteriochlorophyll *a* (BChl *a*) antenna complex of green sulfur bacteria have been the subject of many studies since its high-resolution X-ray structure for *Prosthecochloris aestuarii* was determined in 1974[1] (for recent reviews see refs 2 and 3). This complex is a C_3 trimer of identical subunits that contain seven symmetry inequivalent BChl *a* molecules. Nearest neighbor Mg...Mg distances within a subunit are ∼11−14 Å, and the largest pairwise coupling energies are in the ∼50−200 cm^{-1} range. The largest coupling between BChl *a* molecules belonging to different subunits is ∼20 cm^{-1}. Recently, the X-ray structure of the FMO complex from *Chlorobium tepidum* was determined.[4] The relative orientations of the BChl *a* molecules and the distances between them are very similar to those of *P. aestuarii*. (Some potentially significant differences in H-bonding and BChl *a*−residue distances were observed.) It is interesting, therefore, that the 4.2 K Q_y-absorption spectra of the FMO complex from the two species show significant differences (Figure 1). These differences are most likely due mainly to differences in the excitation energies of one or more of the BChl a molecules of the subunit.[5]

Pearlstein and co-workers (ref 6 and refs therein) recognized early on that the FMO complex is an attractive system for studying excitonic (delocalization) effects in photosynthetic complexes. However, and as underscored in ref 2, the FMO complex is not as simple as one would like because the seven BChls of the subunit are energetically inequivalent and there is no reliable method for calculating their site excitation energies. The calculations of Pearlstein,[6] and later those of Gülen[7] and Louwe et al.,[8] indicated that the Q_y-states are mini-excitons with excitation shared by two or three molecules at most. However, the site excitation energies used in those works were different; for example, the lowest excitation energy was assigned to BChl 7, BChl 6, and BChl 3 (as defined in ref 1), respectively. At present, the model of Louwe et al.[8] appears to be the most reliable on the basis of fits to the absorption, circular dichroism (CD), linear dichroic (LD), and triplet−singlet optical spectra at low temperatures.[5,9] Based on physically reasonable estimates of the energetic inequivalence of C_3-symmetry related BChl molecules belonging to different subunits, it was concluded that the couplings between molecules belonging to different subunits are too weak (≤10 cm^{-1}) to warrant consideration of trimer states. That is, excitation by light resides, to a large extent, on the individual subunits.[8]

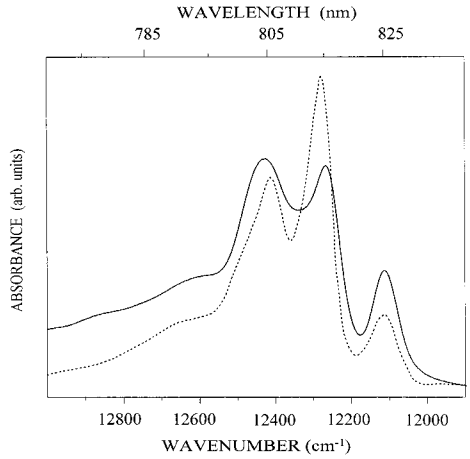

Figure 1. The 4.2 K Q_y-absorption spectra of the FMO trimer complex from *P. aestuarii* (dotted) and *Cb. tepidum* (solid).

Of relevance to this paper is that the 825 nm absorption band, (Figure 1) appears to be due to a Q_y-state mainly localized on

* Corresponding author.
† Iowa State University.
‡ Arizona State University.

10.1021/jp990918g CCC: $18.00
Published on Web 06/19/1999

a single molecule of the subunit, most likely BChl 3. That this band is predominantly inhomogeneously broadened was first established by nonphotochemical hole burning (NPHB) experiments at 4.2 K[10,11] (see also ref 12). The hole spectra[10,11] revealed that the 825 nm band is contributed to by two states separated by ~40 cm^{-1}, a result that was later confirmed by different spectroscopic measurements.[13] The interpretation given in ref 11 for the two contributing states was that they are delocalized excitonic components of the trimer A and E symmetry. In light of the results of Louwe et al.,[9] this assignment now seems unlikely. Rather, it is more probable that the 825 nm band is due to the lowest energy Q_y-state of the subunit with structural heterogeneity leading to the excitation energies of this state in the three subunits of the trimer being different.[8] This view was adopted in a recent Stark hole burning study of the 825 nm band.[14] In this paper, results for the FMO complex from *Cb. tepidum* are presented that support this description of the 825 nm band. Of equal importance is that the dependence of the homogeneous width of the zero-phonon hole (ZPH) on the burn frequency (ω_B) within the 825 nm band leads to time constants for downward excitation energy transfer between the just-mentioned energetically inequivalent states of the trimer. Hole growth kinetic data are presented that are consistent with the homogeneous widths of the ZPH burned into the three states that contribute to the 825 nm band as well as the lifetimes of these states. The dephasing times (T_2) and their temperature dependencies in the 1.8−10 K range are compared with those obtained by Louwe and Aartsma for the FMO complex of *P. aestuarii* using the accumulated photon echo technique.[15]

2. Experimental Section

Absorption and hole-burned spectra were measured by fluorescence excitation spectroscopy using a Coherent CR 899−29 Autoscan Ti:Sapphire laser (line width, <20 MHz) pumped by a 15 W Coherent Innova 200 Ar-ion laser. Laser intensity was stabilized using an LS 100 power stabilizer (Cambridge Research and Instrumentation). Fluorescence was detected and processed by a GaAs photomultiplier tube (Hamamatsu) and a photon counter (SR-400, Stanford Research Instruments). Rejection of scattered laser light was achieved with two long wavelength-pass filters RG 850 and a broad band interference filter P60−940 (Coherent-Ealing). This combination allowed for fluorescence detection between ~910 and 930 nm. Laser intensities used for hole burning were in the range ~20 to 400 $\mu W/cm^2$, depending on the burn wavelength and temperature (see Figure captions). Hole depths were in the range 10−20%. For hole reading, the laser was attenuated by a factor of 10−100. Holes were recorded in 300 s. For the hole growth kinetic studies, burn intensities in the range 40−1600 $\mu W/cm^2$ were used. Hole growth was monitored by measuring the decrease in the fluorescence signal. The total burning time was typically 1000 s. Because the fluorescence decreases rapidly during the first several seconds, the typical channel time used during this period was 0.1 s. After 30 s, when approximately half of the burning was completed, a channel time of 1 s was used.

Samples of the FMO complex from *Cb. tepidum* were prepared as in Savikhin et al.[16] The complexes were dissolved in a glycerol:water solvent (70:30, v/v) containing 20 mM Tris/HCl buffer (pH = 8.0) and contained in a gelatin capsule with a 5 mm optical path length. The optical density of the sample was adjusted to ~0.1 at the 825 nm absorption band at 1.8 K. A Janis 10 DT liquid helium cryostat was used for measurements in the 1.8−10 K range. Temperatures were measured with a silicon diode and temperature controller (model 330, Lakeshore Cryotronics).

TABLE 1: Characterization of Zero-Phonon Holes Burned into the 825 nm Band of the FMO Complex

Burn Wavelength (λ_B) Dependence at 1.8 K

λ_B (nm)	823.0	824.0	825.1	826.0	827.0	828.0
hole width (cm^{-1})[a]	0.32	0.16	0.13	0.075	0.046	0.038
fractional hole depth[b]	0.3		0.49		0.65	
(burn fluence, J/cm^2)	(800)		(200)		(40)	

Temperature Dependence and Lifetimes (this work)

λ_B (nm)[c]	T_1(ps)[d]	A (cm^{-1} $K^{-\alpha}$)[e]	α[f]
827.0	(2×10^3)[g]	0.007	1.3
825.0	117	0.007	1.3
823.0	37	0.007	1.3

Temperature Dependence and Lifetimes (ref 15)

827	2×10^3	0.003	1.3
826	135	0.015	1.3
824	32	0.07	1.3

[a] All holewidths given in this paper were measured for fractional hole depths <0.15. [b] These results are only meant to indicate that the hole burning efficiency decreases significantly as λ_B is tuned from the low energy to high energy side of the 825 nm band. The results of Figures 4a and b allow for quantitative analysis of the λ_B dependence (cf. text). [c] The 827.0, 825.0, and 823.0 nm wavelengths correspond to the locations of the three lowest energy Q_y-states of the FMO complex. [d] T_1 is the lifetime of the excited state (τ in eq 2). Γ_0 in eq 1 equals $(\pi T_1 c)^{-1}$, where c is the speed of light (cm s^{-1}). [e] See eq 1. [f] The value of 1.3 was determined from the $\lambda_B = 827.0$ nm data in Figure 3. [g] Determined from the results in Figure 4 (cf. text). This value is in agreement with the value reported in ref 15 for *P. aestuarii*.

3. Results and Discussion

Temperature and Wavelength Dependencies of Holes in the 825 nm Band of *Cb. tepidum*. Prior to temperature-dependent studies of the ZPH burned at different burn wavelengths (λ_B), holes were burned at 1.8 K at λ_B values between 823.0 and 828.0 nm (top of Table 1). The ZPH profiles (fractional absorbance change, $\lesssim$0.1) were well described by a Lorentzian. The holewidths (fwhm) monotonically increase from 0.038 cm^{-1} at 828.0 nm (red edge of the 825 nm band) to 0.32 cm^{-1} at 823.0 nm (blue edge), as shown in Table 1. This result is qualitatively consistent with the accumulated photon echo (APE) data for *P. aestuarii* of Louwe and Aartsma obtained using 2 ps pulses.[15] It was also observed that the hole burning efficiency decreases significantly as λ_B is tuned from the red to blue sides of the 825 nm band. For example, burn fluences of 800, 200, and 40 mJ/cm^2 at $\lambda_B = 823.0$, 825.1, and 827.0 nm, respectively, produced fractional absorbance changes of 0.33, 0.49, and 0.65, respectively (Table 1). The hole burning efficiency depends sensitively[17] on the induced absorption rate, which is inversely proportional to the homogeneous width of the zero-phonon line (ZPL), and the lifetime of the excited state undergoing hole burning. With this in mind, the hole width results just presented and the data related to hole burning efficiency appear to be correlated. (In the following subsection we show that the holewidth and growth kinetics are entirely consistent.) The three ZPH profiles in Figure 2 exhibit signal-to-noise ratios that are typical of those obtained previously.

As discussed in the Introduction, recent experimental results on the FMO complex strongly indicate that the 825 nm band is contributed to by three transitions that correspond to the lowest energy state of the three subunits. Because of protein structural heterogeneity, the energies of this state in these subunits are

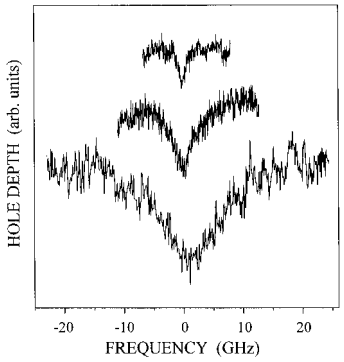

Figure 2. Typical experimental zero-phonon hole profiles from burning into the 827 nm (top), 825 nm (middle), and 823 nm (bottom) states of the FMO complex from *Cb. tepidum*; burn temperature = 1.8 K. Fractional hole depths used to obtain the data in Figure 3 were <0.1.

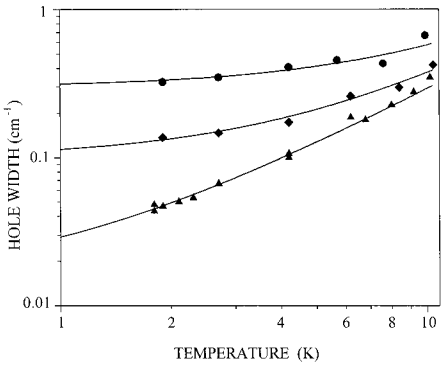

Figure 3. Temperature dependencies of the zero-phonon hole width for burn wavelengths (λ_B) = 823.0 nm (circles), 825 nm (diamonds), and 827.0 nm (triangles). These wavelengths correspond to the three lowest energy states of the FMO complex from *Cb. tepidum*. The solid curves are fits obtained using eq 1.

different. We found that the 825 nm absorption band of *Cb. tepidum* can be fit reasonably well by three equi-intense Gaussians of width 55 cm^{-1} centered at 823.0, 825.0, and 827.0 nm. This fitting corresponds to an average spacing of ~25 cm^{-1} between adjacent levels. A somewhat improved fit to the 825 nm band could be obtained by using three slightly asymmetric profiles with the asymmetry due to electron−phonon coupling as determined in ref 11. Figure 3 shows the temperature dependencies of the widths of holes burned at 823 (circles), 825 (diamonds), and 827 nm (triangles) between 1.8 and 10.0 K. That the temperature dependence of the 823 and 825 nm holewidths is considerably weaker than that of the 827 nm holewidth, especially below ≈4 K, suggests that the widths of the former two holes at 1.8 K are dominated by a temperature-independent contribution, one that we will attribute to downward energy transfer. Preliminary analysis of the 827 nm data points showed that they approximately follow a T^{α} dependence with $\alpha \sim 1.3$. This power law is unique to pure dephasing/spectral diffusion due to two-level systems (TLS) of glasses and proteins.[18−21] Such a temperature dependence has recently been reported for the lowest energy Q_y-state of the photosystem II reaction center[22] and of the LHC II antenna complex of photosystem II,[23] as well as the lowest exciton level of the B850 molecules in the LH2 antenna complex of purple bacteria.[24] However, the hole widths for λ_B = 827 nm are not solely determined by the TLS. This follows because of the apparent convergence of the holewidths for the three burn wavelengths at higher temperatures (Figure 3). That is, if the 827 nm holewidths were due only to TLS, they should add to the energy transfer contributions to the widths of the 823 and 825 nm holes. The transfer kinetics can safely be assumed to be temperature independent for $T \lesssim 10$ K.[25] This line of argument becomes convincing when the hole widths in Figure 3 are fit by

$$\Gamma_{\text{hole}}\,(\text{cm}^{-1}) = \Gamma_0 + 2AT^{\alpha} \qquad (1)$$

where Γ_0 is temperature independent and the second term is due to TLS-induced spectral dynamics. The 827 nm data were fit first (solid curve in Figure 3) and the following values were found: $\Gamma_0 = 0.015$ cm^{-1}, $\alpha = 1.3$, and A = 0.007 (Table 1). Addition of a thermally activated term to eq 1 led to no significant improvement in the fit as expected from the APE results of Louwe and Aartsma[15] that thermally activated dephasing is negligible below ≈10 K. For the 825 and 823 nm holes, α was fixed at 1.3, leaving Γ_0 and *A* as the only adjustable parameters. The values of Γ_0 and *A* obtained from the fits shown in Figure 3 are given in Table 1. That the *A* values obtained for the 823, 825, and 827 nm holes are equal (0.007) is strong evidence for the validity of our analysis because one expects that the spectral dynamics from TLS should be the same for the three subunits of the trimer. For comparison, the results from APE experiments by Louwe and Aartsma[15] on the FMO complex of *P. aestuarii* are also given in Table 1. Although the α values of 1.3 agree with ours, their *A* values for excitation at 824, 826, and 827 nm differ significantly. As already implied, there is no physical basis we can think of for the spectral dynamics from TLS in the three subunits to be different. It should be noted, however, that their fits were obtained from APE data in the 5−30 K range and that above ≈10 K, thermally activated dephasing becomes important. By 30 K, thermally activated dephasing dominates the TLS dynamics. From the data in Figure 3 it is apparent that, in the absence of data points below 5 K, the characterization of the TLS spectral dynamics would become quite uncertain.

The results in Figure 3 and Table 1 are clearly consistent with the model that has the 825 nm band contributed to by the lowest energy state of the three energetically inequivalent subunits of the trimer. We consider next the kinetics of downward energy transfer from the states centered near 823 and 825 nm. This investigation requires an assessment to what the Γ_0 value of 0.015 cm^{-1} for the lowest energy state at ~827 nm is due (Table 1). This Γ_0 value, when viewed as being due to radiative decay, corresponds to a fluorescence lifetime of 706 ps. [The holewidth is twice the homogeneous width of the ZPH, whose width in reciprocal centimeters is given by $(2\pi\ T_1 c)^{-1}$ when pure dephasing is negligible. Here, *c* is the speed of light in units of cm s^{-1} and T_1 is the lifetime.] The APE data,[15] when interpreted in the same way, lead to a T_1 value of 420 ps, about twice as short as the 706 ps value. Aware of the earlier fluorescence decay data of the FMO complex at 77 K, which led to a fluorescence lifetime of 3 ns,[26] Louwe and Aartsma performed pump−probe experiments. The results of these studies led to a fluorescence lifetime of 2 ns for the lowest energy state of the FMO complex at 5 K.[15] This lifetime leads to a contribution of 0.005 cm^{-1} to the Γ_0 value of 0.015 cm^{-1} for the 827 nm state, leaving ~0.010 cm^{-1} to be explained. This residual width could be due to spectral diffusion that occurs on a time scale longer than the fluorescence lifetime and/or some hole burning of the 825 nm band in its low energy wing. In any event, when 0.010 cm^{-1} is subtracted from the Γ_0 values for the 823 and 825 nm states, one arrives at T_1 values for them of 37 and 117 ps, respectively (Table 1). These lifetimes are in reasonable agreement with those determined for *P. aestuarii* by the APE technique at 826 and 824 nm[15] (Table 1). As in that work, we attribute the lifetimes just mentioned to downward

energy transfer. The 823 nm state has two energy transfer pathways, one to the 827 nm state and the other to the 825 nm state. Because the energy gap (25 cm^{-1}) for 825 nm → 827 nm transfer is equal to that for 823 nm → 825 nm transfer, it is reasonable to assume that the rate constant for the former transfer is equal to that for the latter transfer which is $(117\ ps)^{-1}$. Because the rate constant for depopulation of the 823 nm state is $(37\ ps)^{-1}$, it then follows that the rate constant for the 823 nm → 827 nm transfer pathway is $(54\ ps)^{-1}$. The rate constant of $(54\ ps)^{-1}$ is for an energy gap of 50 cm^{-1} and the rate constant of $(117\ ps)^{-1}$ is for a gap of 25 cm^{-1}. Furthermore, the electronic coupling matrix elements for the two transfer processes can be taken to be equal. Thus, it appears that the effective density of states (spectral density) in Fermi's golden rule rate expression for the 823 nm → 827 nm transfer is about a factor of 2 larger than for the 823 nm → 825 nm transfer.

Nonphotochemical Hole Growth Kinetics in the 825 nm Band. The kinetics of nonphotochemical hole growth in amorphous solids are typically quite highly dispersive due to structural heterogeneity.[17,27] Success has been achieved in modeling dispersive hole growth by assuming that the TLS parameters that govern the rate of tunneling in the rate-determining step of hole formation are subject to a Gaussian distribution. This form of distribution for TLS asymmetry and tunneling parameter has been successful in explaining numerous anomalous glass properties. With regard to hole growth, this model leads to the following form for the time-dependent hole depth, $D(t)$:[27]

$$D(t) = (2\pi)^{-1/2} \int_{-\infty}^{\infty} dx \exp[-x^2/2] \exp[-\Sigma_0 \xi(x) t] \quad (2)$$

where $\Sigma_0 = P\sigma\Omega_0\tau$, P is the burn photon flux, σ is the peak absorption cross section, τ is the excited-state lifetime, Ω_0 is the average harmonic frequency of the extrinsic TLS, TLS_{ext}. The TLS_{ext} are glass bistable configurations formed by interaction of the probe molecule with the glass. The integration variable $x = (\lambda - \lambda_0)/\sigma_\lambda$ and $\xi(x) = \exp[-2(\lambda_0 - \sigma_\lambda x)]$. The symbol λ is the tunnel parameter for the TLS_{ext}. Equation 2 is derived by assuming that λ has a Gaussian distribution centered at λ_0, with a standard deviation σ_λ for the TLS_{ext}. The most detailed studies of dispersive hole growth kinetics were performed on Oxazine 720 in glycerol glasses and poly(vinyl alcohol) films[17] and Al-phthalocyanine tetrasulfonate in glassy films of water.[28] In those works, eq 2 was used to establish consistency of the excited-state lifetimes (τ) and temperature-dependent homogeneous widths of the ZPL with the growth kinetics. Here, we establish this consistency for the 825 nm band of the FMO complex. To the best of our knowledge, this is the first time hole growth data have been reported for a photosynthetic complex. The data for $\lambda_B = 823.0$, 825.0, and 827.0 nm obtained at 1.8 and 9.0 K are the noisy curves of Figure 4. The smooth curves are the fits obtained using eq 2. These curves are considered good because the parameter values used to fit any one of the six growth curves could be used to fit the others by an experimentally determined scaling procedure. With reference to eq 2, the lifetimes (τ) and temperature dependence of the homogeneous width (γ) of the ZPL for the states at the aforementioned wavelengths were determined in the preceding subsection (Table 1). The relative values of σ for the three states at any temperature in the 1.8−9.0 K range are known because σ is inversely proportional to γ. In fitting the growth curve for a particular burn wavelength and temperature, $\sigma\Omega_0$ is adjusted and λ_0 and σ_λ varied to yield the best fit. This fitting requires

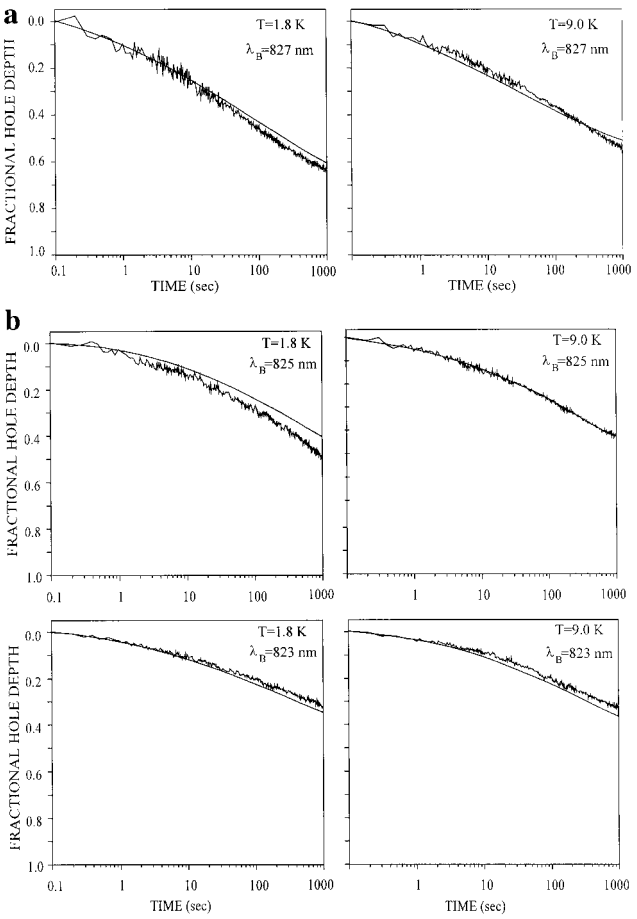

Figure 4. (a) Nonphotochemical hole growth kinetics for the 827 nm state of the FMO complex from *Cb. tepidum* at 1.8 and 9.0 K (noisy curves). The solid curves are fits obtained using eq 2 with $\lambda_0 = 9.6$ and $\sigma_\lambda = 2.3$. Burn fluences used for the 1.8 and 9.0 K experimental hole growth curves were 40 and 160 mJ/cm^2, respectively. See text for discussion of fitting procedure. (b) Nonphotochemical hole growth kinetics for the 825 and 823 nm states of the FMO complex from *Cb. tepidum* at 1.8 and 9.0 K (noisy curves). Solid curves are fits obtained using eq 2 with $\lambda_0 = 9.6$ and $\sigma_\lambda = 2.3$. For $\lambda_B = 825$ nm, the burn fluences for 1.8 and 9.0 K curves were 200 and 400 mJ/cm^2, respectively. For $\lambda_B = 823$ nm, the burn fluences for 1.8 and 9.0 K were 800 and 1600 mJ/cm^2, respectively.

a value for the Huang−Rhys factor S because the maximum fractional absorbance change due to ZPL is given by $\exp(-S)$.[29] We used $S = 0.3$ from ref 11. (For detailed discussion see ref 17.) For fitting of the remaining growth curves, λ_0 and σ_λ are fixed at the values determined by the first fit, and the absorption cross section and burn photon flux (P) values are changed according to the experimental conditions and results shown in Figure 3 and Table 1. Thus, there are no adjustable parameters in these fits. We emphasize that there is no physical basis for allowing λ_0, σ_λ, and S to be different for the 823.0, 825.0, and 827.0 nm states because they are associated with the lowest energy state of the subunit and the three subunits of the trimer are symmetry equivalent.

The fits shown in Figure 4 were obtained with $\lambda_0 = 9.6$ and $\sigma_\lambda = 2.3$. It was found that the values of λ_0 and σ_λ did not significantly depend on the initial growth curve chosen for fitting. For example, the values just presented emerged when only the results in Figure 4b were used. We point this out because had the lifetime of the 827.0 nm state, 2 ns,[15] not been known, fitting of the growth curves in Figure 4a would have led to the same lifetime. Concerning the value of 2.3 for σ_λ,

Kenney et al.[17] reported a value of 0.8 ($\lambda_0 = 7.8$) for oxazine 720 in a glycerol glass and Kim et al.[28] a value of 1.1 ($\lambda_0 = 7.6$) for Al-phthalocyanine tetrasulfonate (APT) in hyperquenched glassy films of water. As discussed in detail by Kenney et al., the dispersiveness of the kinetics for $\sigma_\lambda \sim 1$ is still clearly evident in the data. The value of 2.3 corresponds to highly dispersive kinetics.

Next, we consider the deviations between the experimental growth curves and fits in Figure 4. The burn intensities used to obtain the former varied by a factor of 40 (see Figure captions). Furthermore, the γ values, which the absorption cross sections are inversely proportional to, ranged from 1.4 to 20 GHz. It is because of these large variations that we had earlier said that the fits, as a whole, were good. Because some of the fits overestimate whereas others underestimate the growth kinetics, there does not appear to be a systematic and consistent way to significantly improve the fits shown in the Figure. Thus, we think that the deviations are most likely due to experimental uncertainties associated, for example, with the measurements of the burn intensities; that is, γ and $\tau(T_1)$ values.

Mechanistic Aspects of the Nonphotochemical Hole Burning (NPHB). The current mechanism for NPHB in amorphous solids involves a hierarchy of configurational tunneling events that culminate in a structural change in the near vicinity of the chromophore that leads to persistent hole formation.[30,31] The tunneling events, which involve phonon emission, are usually modeled in terms of a distribution of intrinsic two-level systems (TLS_{int}) and of extrinsic TLS (TLS_{ext}) with the latter associated with the chromophore and the inner shell of the host. The TLS_{int} are intimately connected with the excess free volume of the glassy host, explaining, for example, why APT in cubic ice does not exhibit NPHB whereas APT in glassy water is the most efficient NPHB system yet discovered, with an average quantum yield of 0.1 for an APT S_1 lifetime of 3 ns. It is electronic excitation that triggers the tunneling of the TLS_{int} and that is also responsible for the spectral dynamics discussed in this paper. The data in Figure 4 are consistent with this mechanism because they prove that the holes burned into the absorption bands of the 823 and 825 nm states are the result of nonphotochemical hole burning *in* those states. The possibility that the holes are the result of hole burning in the lowest energy state at 827 nm following its efficient population by energy transfer from the 823 and 825 nm states, can be excluded. (The idea here is that the structural change that accompanies hole burning in the subunit of the trimer associated with the 827 nm state is not localized in that subunit but produces secondary structural changes in the other two subunits.) The reason for this result is that the hole growth kinetics would involve only one lifetime, that of the 827 nm state (2 ns). It is not possible to fit the hole growth data with that single lifetime. Rather, one needs to take into account both the lifetimes and induced absorption rates of the three states (results not shown).

Rejection of the energy transfer based mechanism just mentioned also means that the phonons created in the downward energy transfer processes do not make a significant contribution to hole burning because, again, the hole growth kinetics would be independent of the lifetimes of the 823 and 825 nm states. We mention this because Franken et al.[12] recently suggested that satellite features in the hole spectra of the FMO complex from *P. aestuarii* are the result of structural changes produced by phonons created by relaxation (radiative and nonradiative) of the 827 nm state to the ground state. The satellite features, which were first reported in refs 10 and 11, are broad holes that mirror the higher energy absorption bands when the burn frequency is located in the lowest energy absorption band at 825 nm. The mechanism proposed by Franken et al. is by no means new (see ref 30 and references therein). Shu and Small[30] argued, based on experimental data, that this mechanism for NPHB is, at best, of minor importance. This mechanism is not clearly evident, for example, in the reaction center of *Rps. viridis*[32] and photosystem II[33] and the LHC II antenna Chl *a*/*b* antenna complex of photosystem II.[34] Johnson and Small[11] attributed the satellite holes to an excitonic correlation effect; that is, the BChl molecules that contribute to the 825 nm band contribute to the partially delocalized states responsible for the higher energy absorption bands. This effect is clearly seen for the special pair of the bacterial reaction center.[32] Another possibility is that the structural change that accompanies hole burning of the lowest state of a subunit spatially extends throughout the subunit.

4. Concluding Remarks

The temperature dependencies of holewidths and hole growth kinetics were used to determine the spectral and energy transfer dynamics of the Q_y-states that contribute to the 825 nm absorption band of the FMO complex from *Cb. tepidum*. The strong dependence of the holewidth and hole growth kinetics on the location of the laser excitation frequency in the 825 nm band, when viewed in terms of earlier works, leads to the conclusion that this band is contributed to by three states located at 823, 825, and 827 nm. These states are assigned to the lowest energy state of the subunit of the trimer with their energetic inequivalence due to structural heterogeneity. It should be noted that this assignment is really the same as that given by Johnson and Small in 1991.[11] In that work, the authors attributed the 825 nm band to two states of the trimer that originate from the lowest energy state of the subunit and carry A and E symmetry. They pointed out that structural heterogeneity would split the E state into two components. The nature and resolution of their experiments did not allow for resolution of a third state. It was later that the problem of excitonic localization due to energy disorder received serious attention. According to Louwe et al.,[9] the lowest energy state of the subunit is mainly localized on BChl 3 in *P. aestuarii*. Vulto et al.[5] drew the same conclusion for *Cb. tepidum*. Our finding that the spectral dynamics due to the protein two-level systems are identical for the three states is consistent with their being due to the same state of the subunit. That Louwe and Aartsma[15] found that the spectral dynamics of the states are markedly different (Table 1) is probably because the lowest temperature used in their experiments was 5 K. In any event, there is no physical basis for asserting that the TLS-spectral dynamics of the three subunits should differ so significantly. Our finding that the spectral dynamics are identical is what we would expect.

Detailed analysis of our data led to a lifetime of 2 ns for the 827 nm state in the low-temperature limit, which is in agreement with the value determined by pump−probe experiments.[15] Lifetimes of 37 and 117 ps for the 823 and 825 nm states, respectively, were attributed to downward, intersubunit energy transfer that culminates in population of the lowest energy state at 827 nm. These lifetimes appear to be in reasonable agreement with those for *P. aestuarii* determined by the accumulated photon echo technique[15] (Table 1). A plausible argument was presented that led to energy transfer time constants of 117 and 54 ps for the 823 nm → 825 and 823 nm → 827 nm pathways, respectively. In our opinion, our results, combined with those of Louwe and Aartsma,[15] provide a complete picture for the energy transfer dynamics of the states associated with the 825

nm band of the FMO complex. What remains to be done are theoretical calculations of the energy transfer rates.

Acknowledgment. Research at the Ames Laboratory was supported by the Division of Chemical Sciences, Office of Basic Energy Sciences, U.S. Department of Energy. Ames Laboratory is operated for USDOE by Iowa State University under contract W-7405-Eng-82. Research at Arizona State University was supported by Grant DE-FG03-97ER20267 from the Energy Biosciences program of USDOE.

References and Notes

(1) Fenna, R. E.; Matthews, B. W.; Olson, J. M.; Shaw, E. K. *J. Mol. Biol.* **1974**, *84*, 231.

(2) Blankenship, R. E.; Olson, J. M.; Miller, M. In *Anoxygenic Photosynthetic Bacteria*; Blankenship, R. E., Madigan, M. T., Bauer, C. E., Eds.; Kluwer: Dordrecht, 1995; pp 399−435.

(3) Savikhin, S.; Buck, D. R.; Struve, W. S. *J. Phys. Chem. B.* **1998**, *102*, 5556.

(4) Li, Y. F.; Zhou, W.; Blankenship, R. E.; Allen, J. P. *J. Mol. Biol*. **1997**, *271*, 456.

(5) Vulto, S. I. E.; de Baat, M. A.; Louwe, R. J. W.; Permentier, H. P.; Neef, T.; Miller, M.; van Amerongen, H.; Aartsma, T. *J. Phys. Chem. B.* **1998**, *102*, 9577.

(6) Lu, X.; Pearlstein, R. M. *Photochem. Photobiol*. **1993**, *57*, 86.

(7) Gülen, D. *J. Phys. Chem.* **1996**, *100*, 17684.

(8) Louwe, R. J. W.; Vrieze, T.; Hoff, A. J.; Aartsma, T. J. *J. Phys. Chem. B* **1997**, *101*, 11280.

(9) Louwe, R. J. W.; Vrieze, T.; Aartsma, T. J.; Hoff, A. J. *J. Phys. Chem. B.* **1997**, *101*, 11273.

(10) Johnson, S. G.; Small, G. J. *Chem. Phys. Lett*. **1989**, *155*, 371.

(11) Johnson, S. G.; Small, G. J. *J. Phys. Chem.* **1991**, *95*, 471.

(12) Franken, E. M.; Neerken, S.; Louwe, R. J. W.; Amesz, J.; Aartsma, T. J. *Biochemistry* **1998**, *37*, 5046.

(13) Louwe, R. J. W.; Aartsma, T. J. *J. Lumin*. **1994**, *58*, 154.

(14) Rätsep, M.; Wu, H.-M.; Hayes, J. M.; Blankenship, R. E.; Cogdell, R. J.; Small, G. J. *J. Phys. Chem. B.* **1998**, *102*, 4035.

(15) Louwe, R. J. W.; Aartsma, T. J. *J. Phys. Chem.* **1997**, *101*, 7221.

(16) Savikhin, S.; Zhou, W.; Blankenship, R. E.; Struve, W. S. *Biophys. J*. **1994**, *66*, 110.

(17) Kenney, M.; Jankowiak, R.; Small, G. J. *J. Chem. Phys*. **1990**, *146*, 47.

(18) Völker, S. In *Relaxation Processes in Molecular Excited States*; Fünfschilling, J., Ed.; Kluwer: Dordrecht, 1989; p 113.

(19) Narasimhan, L. R.; Littau, K. A.; Pack, D. W.; Bai, Y. S.; Elscher, A.; Fayer, M. D. *Chem. Rev.* **1990**, *90*, 439.

(20) Hayes, J. M.; Jankowiak, R.; Small, G. J. In *Topics in Current Physics, Vol. 44, Persistent Hole Burning: Science and Applications*; Moerner, W. E., Ed.; Springer: Berlin, 1988; p 153.

(21) Hayes, J. M.; Jankowiak, R.; Small, G. J. *Chem. Rev.* **1993**, *93*, 1471.

(22) den Hartog, E. T. H.; Vacha, F.; Lock, A. J.; Barber, J.; Dekker, J. P.; Völker, S. *J. Phys. Chem. B.* **1998**, *102*, 9174.

(23) Pieper, J.; Rätsep, M.; Jankowiak, R.; Irrgang, K.-D.; Voigt, J.; Renger, G.; Small, G. J. *J. Phys. Chem. A* **1999**, *103*, 2412.

(24) Wu, H.-M.; Rätsep, M.; Lee, I.-J.; Cogdell, R. J.; Small, G. J. *J. Phys. Chem. B* **1997**, *101*, 7654.

(25) At 10 K, $kT = 6.9\ \mathrm{cm}^{-1}$. The rate of downward energy transfer for an energy gap of $25\ \mathrm{cm}^{-1}$ should be proportional to $n_\omega + 1$, where n_ω is the thermal occupation number of phonons with frequency $\omega = 25\ \mathrm{cm}^{-1}$. At 10 K, $n_\omega = 0.03$.

(26) Freiberg, A.; Lin, S.; Timpmann, K.; Blankenship, R. *J. Phys. Chem. B.* **1997**, *101*, 7211.

(27) Shu, L.; Small, G. J. *J. Opt. Soc. Am. B.* **1992**, *9*, 733.

(28) Kim. W.-H.; Reinot, T.; Hayes, J. M.; Small, G. J. *J. Phys. Chem.* **1995**, *99*, 7300.

(29) Rebane, K. K. *Impurity Spectra of Solids*; Plenum: New York, 1970.

(30) Shu, L.; Small, G. *J. Chem. Phys.* **1990**, *141*, 447.

(31) Shu, L.; Small, G. J. *J. Opt. Soc. Am.* **1992**, *9*, 724.

(32) Reddy, N. R. S.; Kolaczkowski, S. V.; Small, G. J. *J. Phys. Chem.* **1993**, *97*, 6934.

(33) Jankowiak, R.; Tang, D.; Small, G. J.; Seibert, M. *J. Phys. Chem.* **1990**, *94*, 6519.

(34) Reddy, N. R. S.; van Amerongen, H.; Kwa, S. L. S.; van Grondelle, R.; Small, G. J. *J. Phys. Chem.* **1994**, *98*, 4729.